

The 25 cm XIPS[®] Life Test and Post-Test Analysis

IEPC-2009-161

*Presented at the 31st International Electric Propulsion Conference,
University of Michigan Ann Arbor Michigan
September 20-24, 2009*

William G. Tighe*, Kuei-Ru Chien†, Zeke Solis‡, and Rafael Spears§
L-3 Communications Electron Technologies, Inc., Torrance, CA, 90505

Abstract: The Life Test for the 25 cm Xenon Ion Propulsion System (XIPS[®]) thruster has been completed. The Life Test ran for a total of 16,250 hrs and 14,142 cycles. The Q2 Life Test Thruster operated for 2880 hrs and 332 ON/OFF cycles at high power and 13,370 hrs and 13,810 ON/OFF cycles at low power, satisfying the mission requirements for the Boeing 702 class commercial communication satellite. In this presentation we will describe this mission requirement and report on thruster performance parameters. Near the mid-point of the Low Power phase of the Life Test, an anomaly occurred with the discharge cathode heater. This event led to a detailed root cause analysis, corrective action and an independent re-qualification test program for the heater¹. The Discharge Cathode Assembly (DCA) was replaced and the Life Test was continued until voluntarily terminated when the mission requirements were demonstrated. Independently, a 25-cm DCA was life tested² at the Jet Propulsion Laboratory (JPL) and has verified that the unit meets both the Boeing requirements and even more stringent mission requirements required for Deep Space missions. The JPL-DCA life test was voluntarily terminated at 16,200 hrs after successfully demonstrating³ over 5000 hrs at high power and over 5000 hrs at each of two lower power levels. Following the Q2 Thruster Life Test, the thruster was removed from the test chamber and physical analysis was performed. This included careful inspection and photo-documentation of the thruster prior to disassembly and of each of the thruster subsystems and components following disassembly. Careful inspection of the optics and measurements of the grid erosion were made. The grids along with the discharge and neutralizer cathode assemblies (DCA and NCA) underwent Destructive Physical Analysis (DPA) in order to characterize erosion and deposition. The cathode inserts were examined in detail including a systematic evaluation of the pore chemistry to characterize barium depletion. Although no life limiting issues were identified, the NCA Keeper did experience more wear than expected, prompting additional wear testing and modeling so that the component can be demonstrated to meet more stringent life requirements.

1. W. G. Tighe, K. Freick and K.R. Chien, "Performance Evaluation and Life Test of the XIPS Hollow Cathode Heater", AIAA-2005-4066, 41th Joint Propulsion Conference, Tucson, AZ, July 10-13, 2005.
2. J.E. Polk, D.M. Goebel and W. Tighe, "Ongoing Wear Test of a XIPS 25-cm Thruster Discharge Cathode" AIAA-2008-4913, 44th Joint Propulsion Conference, Hartford, CT, July 21-23, 2008.
3. J.E. Polk, D.M. Goebel and W. Tighe, "Results of the Wear Test of a XIPS 25-cm Thruster Discharge Cathode" this IEPC conference.

* Physicist/Engineer, Electric Propulsion, L-3 ETI, william.g.tighe@L-3com.com

† Chief Engineer, Electric Propulsion, L-3 ETI, kuei-ru.chien@L-3com.com

‡ Engineer, Electric Propulsion, L-3 ETI, ezequiel.solis@L-3com.com

§ Vice President, Electric Propulsion, L-3 ETI, Rafael.Spears@L-3com.com

I. Introduction

The 25-cm XIPS[®] thruster, manufactured by L-3 Communications Electron Technologies Incorporated (L-3 ETI) Electric Propulsion Product Line, has low (2 kW) and high (4.25 kW) power modes and is used for both orbit-raising and station-keeping functions on the Boeing 702 communication satellite. In this application 4 thrusters and 2 power supplies make up a single EP system, with full redundancy, on the satellite. To date, 68 25-cm thrusters have been placed in orbit and have accumulated more than 107,000 operational hrs. An additional 8 thrusters are in spacecraft integration and 12 more are in production. A description of the manufacturing and test capability at L-3 ETI has been previously reported [1]. The 25-cm XIPS[®] has been successfully life tested. In this report the Life Test will be summarized and the results of the subsequent thruster evaluation and Destructive Physical Analysis (DPA) will be reported.

The next section provides a brief description of the 25-cm XIPS[®] thruster. Section III will summarize the Life Test, including test requirements and performance results. Section IV will provide details of the DPA with discussion and conclusions in Section V.

II. The 25-cm XIPS[®] Thruster

A cut-away view of the XIPS[®] thruster is shown in Fig. 1. It consists of a cylindrical discharge chamber, a 3-grid optical assembly, and a neutralizer cathode assembly. The discharge chamber plasma is ignited and driven by electrons emitted from the discharge cathode assembly (DCA). The DCA is made up of a hollow cathode insert, a cathode tube and orifice plate, an external heater coil, and a Keeper (see Fig. 2). Electron trajectories in the discharge chamber are determined by electric and magnetic fields associated with the applied discharge voltage (V_d) and the ring cusp B-field generated by 3 rings of permanent magnets. The discharge chamber is constructed of iron with a stainless steel liner used to trap material deposited on the chamber wall and prevent it from flaking off.

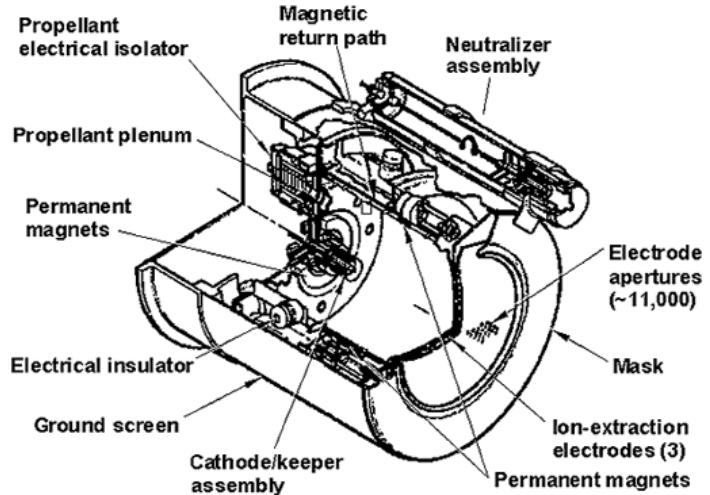


Figure 1. A cut-away view of the XIPS[®] Thruster

The Neutralizer Cathode Assembly (NCA) is basically identical to the DCA and is used to provide an electron beam that exactly balances (or neutralizes) the ion beam current. This prevents the spacecraft from charging up due to the ejection of positive ions in the thruster beam.

In the XIPS[®] thruster, the total neutral xenon gas flow is determined by a temperature controlled orifice. From here it is distributed through a manifold to the main discharge chamber and to both the discharge and the neutralizer cathode assemblies. These three flows are set by fixed orifices that are precisely selected to provide the desired performance. The hollow cathode assemblies require the neutral xenon gas to produce plasma between the cathode orifice and the Keeper. This plasma heats the cathode insert directly through ion and electron bombardment and eliminates the space-charge limitations on thermionic emission allowing the required electron current to produce either the main discharge plasma or the neutralizing electron beam.

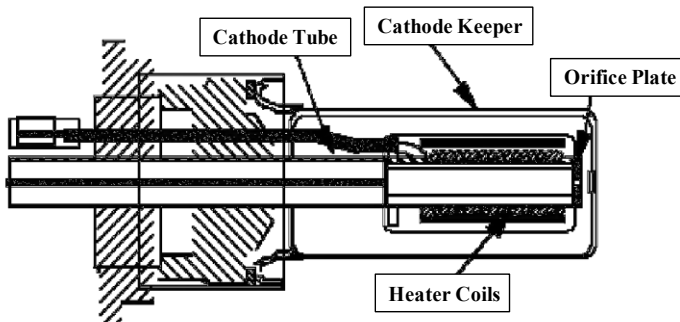


Figure 2. Schematic of the Cathode Assembly

A possible life limiting processes for the ion thruster is associated with the depletion of barium from the hollow cathode insert. This could eventually prevent the cathode from igniting and, in turn, the thruster from operating. Successful cathode ignition is of particular importance in the XIPS[®] thruster since, in their primary role of station-keeping, the cathodes need to be ignited every day. A detailed cathode ignition and life model has been developed at L-3 ETI in an effort to better understand the ignition process and accurately predict the cathode life [2, 3].

The XIPS[®] Optics Assembly consists of three grids: the Screen, the Accel and the Decel grid. Each grid on the 25 cm thruster has ~11000 holes and the 3 grids need to be precisely aligned for efficient beam extraction and to minimize ion impact and erosion of the grid web structure. The Screen is the innermost grid and is effectively an outer wall of the discharge chamber. The Accel grid is used to extract and accelerate xenon ions from the discharge chamber. The Decel grid acts to protect the Accel grid from excessive erosion from returning beam ions. A basic wear mechanism involves the erosion of the Accel grid holes to a diameter that no longer prevents the backstreaming of electrons into the screen grid that shuts down the beam voltage and stops the thruster operation. Erosion of the Screen and the Accel grid web material to a point that causes failure of this support structure can also lead to the failure of the thruster. The presence of the Decel grid reduces these wear mechanisms and provides longer grid life [4].

The 25-cm XIPS[®] performance characteristics are summarized in Table 1. The discharge plasma and the thruster ion beam characteristics have been carefully mapped out using ExB, Thrust Vector, Langmuir and Faraday probes.

The power processor unit is called the XIPS[®] Power Controller (XPC). The XPC controls the thruster and interfaces with the spacecraft. The XPC takes the bus power provided by the satellite and conditions it to the power levels that the thruster needs. A single XPC operates a pair of north-south ion thrusters independently. As a system interface, the XPC provides timing and sequencing for thruster on and thruster off commands, performs fault protection to avoid damage to the thruster and any of the spacecraft components, performs grid clearing in the case of a particle or a flake being caught between two of the electrode grids and, finally, it provides telemetry for the purpose of measuring thruster performance. Table 2 summarizes typical performance characteristics of the XPC.

Following manufacture, the 25-cm thruster undergoes a standard Acceptance Test Procedure (ATP) that consists of an initial 20 hr conditioning, 4 thermal cycles, a vibration test and 4 additional thermal cycles. Total operating time in ATP is typically between 150 – 200 hrs. The majority of testing is at High Power but both High and Low Power Functional Tests are performed during ATP.

Table 1. 25-cm XIPS[®] Ion Thruster Performance

Parameter	Low Power	High Power
Total Input Power (W)	2067	4215
Thrust (mN)	79	165
Specific Impulse (s)	3400	3500
Electrical Efficiency (%)	87	87
Mass Utilization Efficiency (%)	82	84
Beam Voltage (V)	1215	1215
Beam Current (mA)	1.43	3.01
Mass (kg)	13.7	same

Table 2. 25-cm XIPS[®] Power Controller Performance

Parameter	Low Power	High Power
Total Input Power (W)	2200	4500
Bus Input Voltage (V)	100	100
PPU Efficiency (%)	92	94
Size (cm)	20.6x54.1x35.1	same
Mass (kg)	21.3	same

III. Life Test Plan and Performance

A. Test Overview

The 25 cm XIPS[®] Thruster Life Test was conducted in a large (20 x 40 ft), cryogenically pumped vacuum chamber (see Fig. 3) at L-3 ETI in Torrance, California. The chamber has 30, 4 ft cryotubs and is able to pump about 1 million liters of Xe per second. The base pressure for this chamber is $\sim 2 \times 10^{-8}$ torr and with the thruster operating in low power (low flow), the chamber maintains a pressure of 1.5×10^{-6} torr and 3.0×10^{-6} torr in high power.

The Life Test was designed to verify that the thruster would meet the Boeing 702 mission requirements. The first mission phase is Orbit-Raising. This involves a maximum expected duration, at high power, of a little more than 1000 hrs per thruster. To accommodate one failure at launch, the high power requirement for the Life Test was set to twice this duration plus margin. During this “High Power” phase of the Life Test, the thruster ON time was set to 23 hrs and the thruster OFF time to 1 hr.

The second mission phase is Station-Keeping. For a typical mission the thruster is expected to operate during this phase at low power for ~ 1 hour every day for ~ 15 years. The Life Test requirement for this “Low Power” phase also accommodated one failure at launch plus margin. To shorten the test duration, the thruster was operated with ~ 1 hr ON time and 30 minutes OFF time, providing 16 cycles per day. To simulate low-power, Station-Change requirements, the Life Test Thruster was also subjected to 20, 40 hr cycles.

A summary of the actual thruster operations during the Life Test is provided in table 3. The Life Test was started following an extended Acceptance Test Program (ATP) that included additional High Power operation indicated in Table 3.

During the High-Power phase the thruster was operated primarily with a test console consisting of standard laboratory power supplies and test equipment and a control and data

acquisition computer. Due to system definitions and control actions, operation of the thruster with a test console resulted in a significant increase in the number of recorded recycles when compared with operations with an XPC. Aside from the high recycle rate, the only significant event to occur during the high-power phase was the need to increase the voltage on the Accelerator grid to avoid back-streaming.

Unlike the High-Power phase, more than 2/3’s of the low-power phase was performed using an engineering model XPC (identical to a flight unit) and a passive In-line Data System (IDS) used to monitor the data provided through telemetry.

The most significant event to occur during the Low-Power phase was a heater anomaly in the DCA. This resulted in a need for abnormal procedures to achieve thruster ignition. It was decided to replace the DCA, perform a Root Cause and Corrective Action (RCCA) approach to the heater anomaly and continue with the Life Test. Details of the subsequent investigation have been reported [5]. It was determined that the anomaly was caused by a deterioration of the heater insulation due to material flaws and high operating temperatures. Corrective action involved a heater re-design and improvements to manufacture, inspection, installation and test, followed by an extensive qualification program. Modeling and additional wear testing [6] have separately qualified the DCA.

Also observed was a rise in the coupling voltage toward the end of the Low Power phase of the Life Test, most likely as a result of Neutralizer Keeper erosion.

In addition to meeting twice the mission duration plus margin, at the customer’s request, the thruster (at various times during the test) was operated with the discharge voltage (V_d) at a high, though still acceptable, level. The impact of high V_d is to increase Screen Grid erosion.



Figure 3. Life Test Chamber used for the Q2, 25 cm XIPS[®] Thruster at L-3 ETI.

Table 3. 25-cm XIPS[®] Life Test Summary

Parameter	ATP	High Power	Low Power	Total
ON time (hrs)	550*	2330	13,370	16,250
Cycles	16	316	13,810	14,142
Xe throughput (kG)	4	40	114	158

* High Power

B. Test Results

During the Life Test the operating parameters recorded are: on-time, chamber pressure, recycle count, discharge current and voltage, discharge keeper current and voltage, beam current and voltage, accelerator grid current and voltage, decelerator grid current, neutralizer keeper current and voltage, coupling voltage, discharge heater current, discharge heater voltage, neutralizer heater current, neutralizer heater voltage and xenon inlet pressure. In addition, the following performance parameters are automatically calculated: flow, thrust, specific impulse, power, electrical efficiency, propellant utilization efficiency and overall thruster efficiency.

The performance of the Q2 thruster during Life Test is followed both by trend plots of the operating and performance parameters and interval functional testing. Trend Plot data was taken minute-by-minute and values taken mid-way during the operating period were plotted. Approximately every 500 hrs, the Life-Test Thruster was subjected to a full thermal cycle (-40 °C to 194 °C) and a functional test.

At each functional test, the thruster was started from an ambient condition (20°C). After 1 hr, the performance of the thruster was characterized by measuring all the operational parameters. In addition, the sensitivity of the thruster was characterized and the backstreaming limit, the perveance, and thrust vector of the thruster were measured. To reduce down time, these tests were performed less frequently after ~8500 hrs of power operation. During the high-power phase, after the initial functional test, four additional functional tests were performed after 500, 1000, 1500 and 2300 hrs of life testing.

Examples of High Power Trend Plots and Functional Test Plots are shown in Figs. 4 to 7. The Thrust and Isp were very stable and well within specification throughout the High Power phase of the Life Test. Due to Accel grid

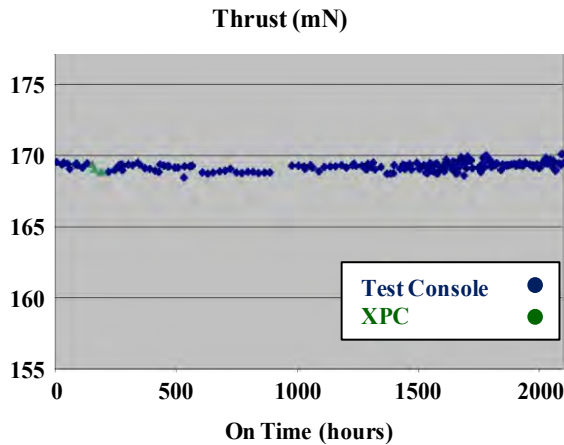


Figure 4. High Power Trend Plot showing Thrust.

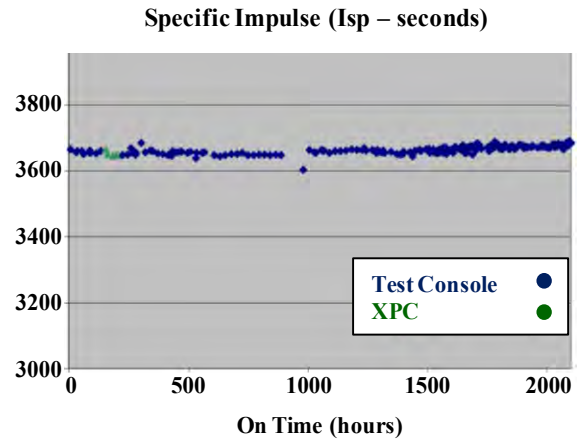


Figure 5. High Power Trend Plot showing Specific Impulse

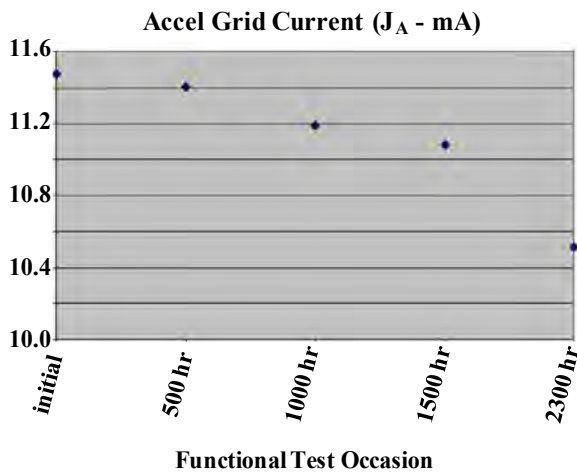


Figure 6. High Power Functional Test Results. Accel Current Measurements

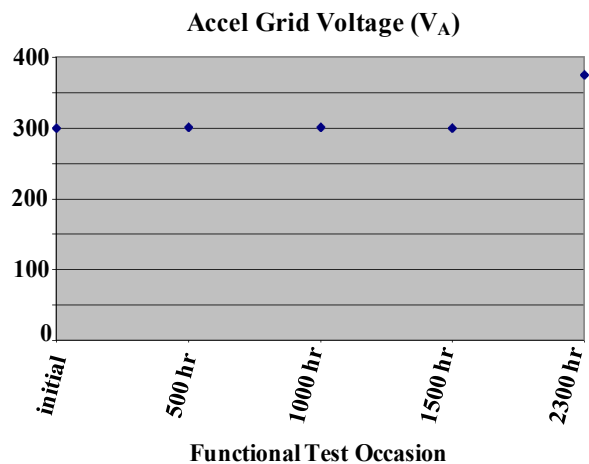


Figure 7. High Power Functional Test Results. Accel Voltage Measurements

aperture diameter enlargement, the Accel grid current decreased during the High-Power phase of testing, and toward the end of this test phase, the Accel voltage had to be increased in order to prevent excess recycles at start up.

At the conclusion of the High-Power phase, the thruster Optics Assembly was removed and closely examined. No evidence of Screen grid wear was detected.

There were a total of 19 functional tests performed during the low-power phase of the life test. All thruster parameters were within specification during all nineteen functional tests. Examples of Trend Plots and Functional Test Plots are shown in Figs. 8 to 11. The intentional change of the gas flow is indicated. The reason for this was to increase the discharge voltage to a “worst case” condition for wear of the Screen grid. In addition the steady increase in the Neutralizer Coupling Voltage (V_g) and the sudden increase in V_g on the last Functional Test Occasion was noted and felt to be due to erosion of the NCA Keeper and Orifice Plate.

With the completion of the Low Power operation, the Life Test was voluntarily terminated. The Q2 thruster successfully demonstrated the required thruster life, ON/OFF cycles, and Xe throughput for the Boeing 702 Class communication satellite. In addition, the thruster met the thrust, thrust level repeatability, specific impulse, thrust vector alignment, beam divergence and propellant utilization requirements.

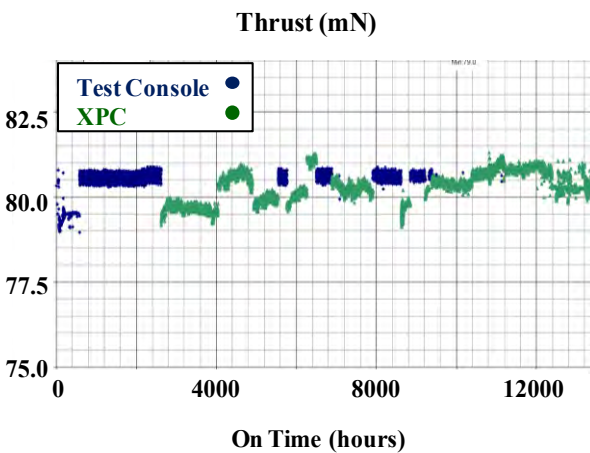


Figure 8. Low Power Trend Plot showing Thrust.

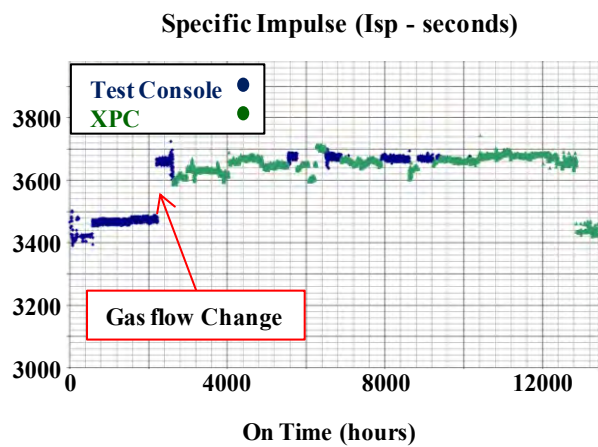


Figure 9. Low Power Trend Plot showing Specific Impulse.

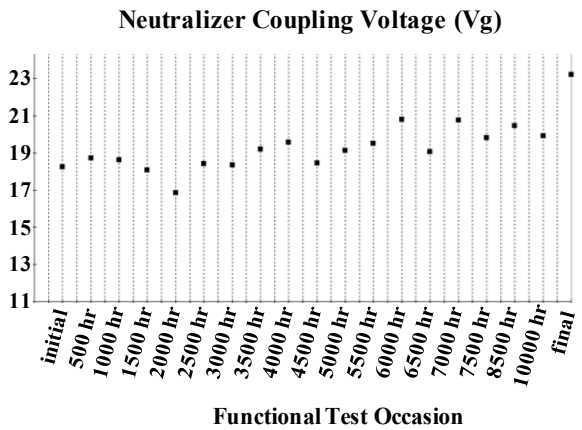


Figure 10. Low Power Functional Test Results showing the Neutralizer Coupling Voltage.

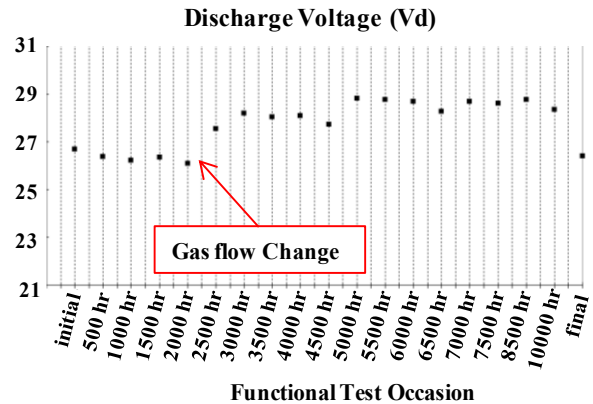


Figure 11. Low Power Functional Test Results showing the Discharge Voltage.

IV. The 25-cm XIPS[®] Q2 Thruster Post-Test Analysis

A. Introduction

This section primarily outlines the Destructive Physical Analysis (DPA) of the 25 cm XIPS[®] Life Test Qualification Thruster, Q2, following successful completion of the Life Test program. As has been mentioned, the Q2 Life Test was voluntarily terminated with the thruster meeting all operating conditions as required by the Boeing 702 Communication Satellite orbit-raising and station-keeping mission. The purpose of the DPA was, therefore, to allow better understanding of all wear mechanisms and to determine if there were any imminent failure conditions. This data will be used to benchmark erosion models that, in turn, can provide predictions for expected life under different mission profiles.

Prior to DPA, photo-documentation of the thruster and the test chamber was completed. The thruster was then transported to a clean room where it was prepared for a series of nondestructive and destructive tests. A procedure to disassemble and prepare the sub-components of the thruster was prepared. Nondestructive analyses included photographs, dimensional, electrical, and mass measurements. Destructive testing required disassembly, cutting, fracturing, potting, polishing, and sectioning. Tests included high-resolution optical and metallographic imaging, Electron Spectroscopy for Chemical Analysis (ESCA), Scanning Electron Microscopy (SEM), and Energy Dispersive Spectra (EDS) for element identification.

All components of the Q2 thruster have been thoroughly investigated and documented. Of necessity only a small fraction of the data and analysis can be included here. The emphasis, in this paper, will be the potential life-limiting components: the grid optics and the cathodes.

The primary findings of this work were: 1) the Accel grid apertures had opened by ~ 50% (requiring higher V_A toward the end of the High-Power phase) but otherwise erosion and deposition patterns of the grids were as expected, and 2) the NCA Keeper was eroded (causing an increase in V_g and V_{NK}) but was not in danger of failure.

B. Grid Optics

The grid optics assembly consists of 3 grids. They are dishd outward with a spherical radius. The innermost grid is the Screen, the central grid is the Accel and the outer grid is the Decel.

A standard set of measurements of the grid optics is made following initial assembly. Aperture diameter, grid spacing, and aperture concentricity are measured with a Z-scope. Dimensions are taken on the complete 3-grid assembly so the Accel aperture size is measured by looking through the outer grids. During the Life Test measurements were repeated following the High Power phase and when the DCA was replaced ~5000 hrs into the Low Power phase of the Life Test. At the termination of the Life Test a final set of measurements was made. Aperture sizes were also measured approximately every 1000 hrs using a camera with a long focal length lens.

An overview photograph of the grid set post-test is shown in Fig.12. A normalized plot of the final grid dimensions (with the original sizes indicated) is provided in Fig. 13.

There has been clear enlargement of the Accel and Decel grid holes, particularly toward the outer radius. The Screen apertures have actually become smaller, presumably due to deposits. It was found that the Accel – Decel separation increased, possibly due to erosion, and the Screen – Accel separation decreased in the mid-radius region suggesting some distortion in the grid shape.



Figure 12. Overview of the Q2 Electrode Grid Set

Because of the size of the grid set, it was felt that any attempt to pot the entire assembly in epoxy would result in significant distortion and invalid interpretation of the relative grid orientation. For this reason, the Optics Assembly was disassembled prior to DPA and each grid was individually photo-documented, weighed and measurements of the grid apertures were repeated.

It was observed that the Decel grid had a few regions near the outer edge where the webbing (the grid material separating the holes) was locally compromised and in some cases lost. There were no occurrences of complete loss of webbing between grid holes on either the Screen or Accel grids and they appeared to be in good shape.

There was single location (shown later) that was the site of damage on all 3 grids.

The analysis of each grid began with careful photo-documentation. In some cases high-resolution optical images were made. Each grid was then potted, sectioned and polished. The potting was performed in stages, with potting compound being allowed to settle and bubbles removed. During this process there was some distortion to the original spherical shape but great care was taken to ensure that the material integrity was maintained.

A pie-shaped section was cut from the potted grid, ground to the central plane of the apertures and then polished. Optical images were taken at the center, mid-radius and edge locations of the polished section. The section was then etched and metallographic images were taken.

The potted, polished section was then analyzed further using a Z-Scope. This instrument was programmed to scan the entire section and locate the edges of each piece of webbing from the center to the outside radius. This produced digital images of the webbing and allowed the webbing width and thickness to be characterized as a function of radial location. The aperture sizes as a function of radius could then be determined from the location of the webbing edges. Finally a small section of the potted section was removed and used to obtain SEM images and elemental analysis of any deposit using EDS analysis. This analysis is on-going and will be reported at a later date.

1. Screen Grid

Photographs of the downstream face and the upstream (flipped) face of the Screen grid are shown in Fig. 14. The downstream face is dished outward and the upstream face is dished inward.

Close-up photographs of a region of the Screen grid that contained a small inclusion in a single aperture are shown in Fig. 15. Except for the inclusion, the photograph is representative of the grid surface.

The presence of hexagonal grooves surrounding the apertures is clearly indicated on the upstream face of the grid. This is probably due to direct erosion of this surface from plasma ions and is similar to the "pits & grooves" erosion observed with the NSTAR thruster[7]. The downstream face is smooth.

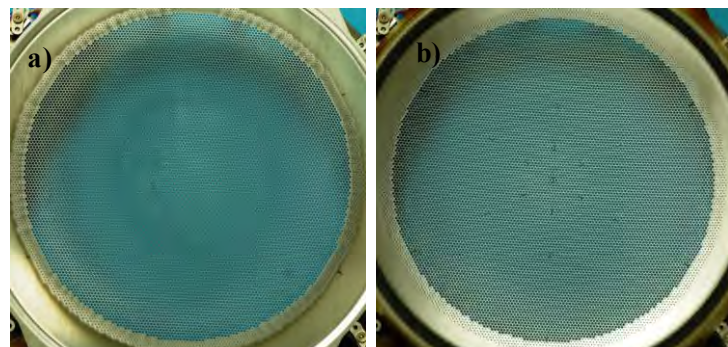


Figure 14. Downstream (a) and upstream (b) face of the Q2 Screen Grid at the end of the Life Test.

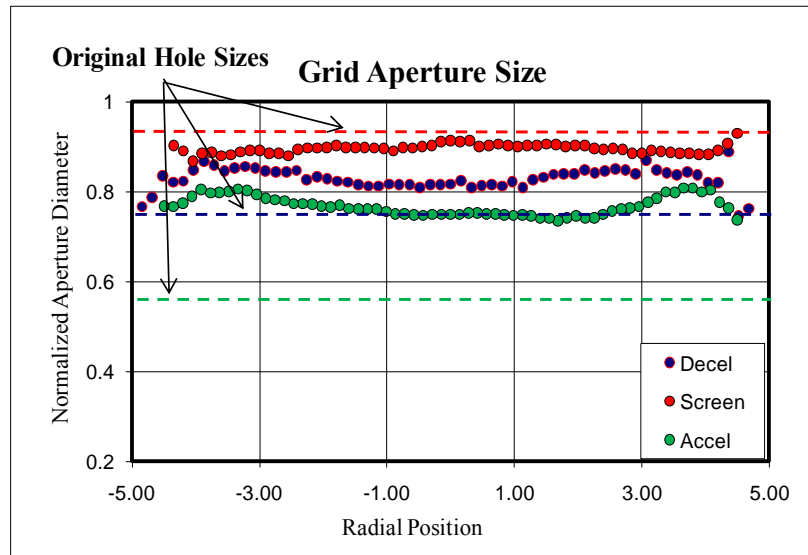


Figure 13. A plot of normalized aperture diameter for the Q2 Grid Set as measured prior to disassembly. Dashed lines indicate the original aperture diameter.

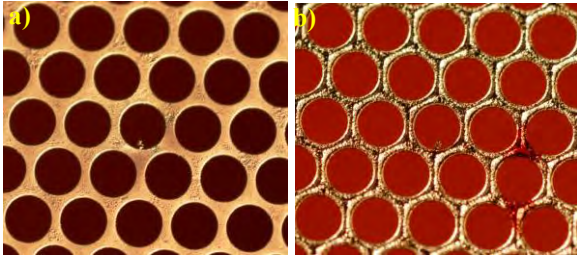


Figure 15. Close-up images of downstream (a) and upstream (b) faces of the Q2 Screen Grid

The Screen grid was then potted, sectioned and polished. Examples of optical and metallographic images are shown in Fig. 17. Significant erosion of the webbing was observed on the upstream face at the center of the grid. This reduced in a fairly linear manner toward the edge. The erosion at the center of the webbing was symmetric, increasing in the regions toward the aperture. From the half radius outward, there was some loss of symmetry to the erosion pattern.

On the edges and on the downstream face of the webbing, there is a significant and fairly uniform layer of deposit. Possibly due to this layer, there is little detectable erosion of the wall of the grid aperture. The original cusped shape of the aperture wall remains clear though eroded from the base of the upstream face.

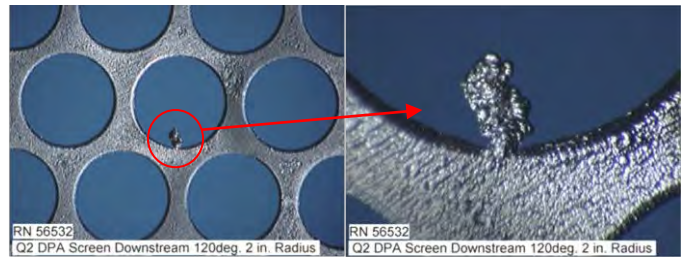


Figure 16. High resolution image of the downstream face of the Q2 Screen grid showing the inclusion.

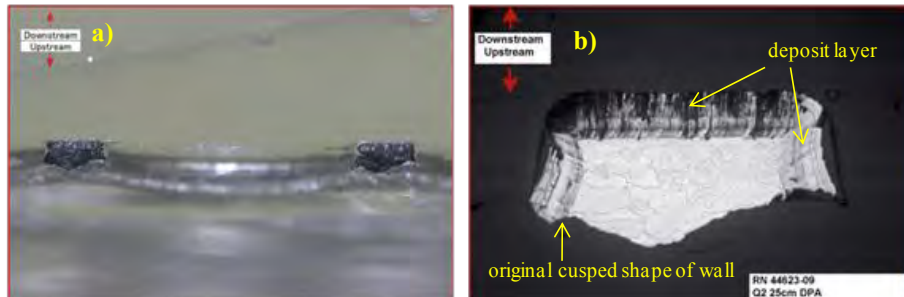


Figure 17. Example of optical (a) and metallographic (b) images of the webbing structure at the aperture mid-plane, mid-radius in the Q2 Screen.

2. Accel Grid

Photographs of the downstream face and the upstream (flipped) face of the Accel grid are shown in Fig. 18. A close-up photograph of a region of the Accel grid that showed some damage in a single aperture is shown in Fig. 19. This is approximately the same region shown for the Screen grid in Fig. 15. Aside from the damaged region, the photograph is fairly representative of the grid surface.

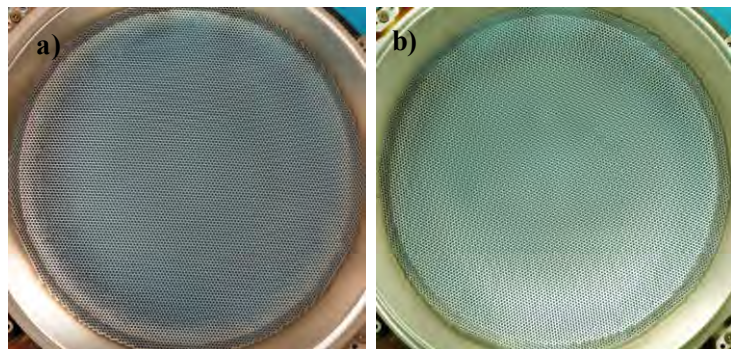


Figure 18. Downstream (a) and upstream (b) face of the Q2 Accel grid.

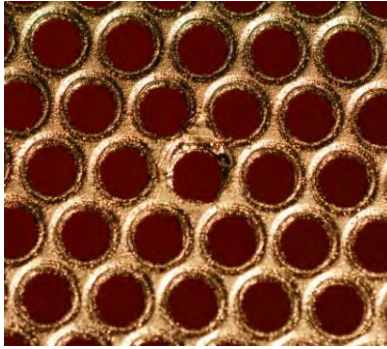


Figure 19. Close-up photo of the downstream face of the Accel grid showing a region of wear.

grid in Fig. 15. Except for the loss of webbing, the photograph is fairly representative of the grid surface.

The hexagonal erosion of the apertures and hexagonal erosion patterns surrounding them was most prominent toward the central region but occurred over the entire face of the grid.

Optical and metallographic images are shown in Fig. 22. There was little change in the grid thickness across the radius. There was a loss of webbing width and, therefore, aperture enlargement across the radius. Analysis has shown that this aperture enlargement increases outward from mid-radius. On the upstream face of the webbing, there was a layer of deposit that became thickest at mid-radius. The erosion of the hole wall was quite uniform in the center with most of the original cusped wall shape (due to the manufacturing process) being lost. At the mid-radius there was greater erosion of the hole wall and there is some asymmetry. At the edge the erosion pattern was very non-symmetric with the cusp feature untouched in the direction of the outside wall but on the other side there was a strongly angled erosion pattern that may reflect the path of beam ions.

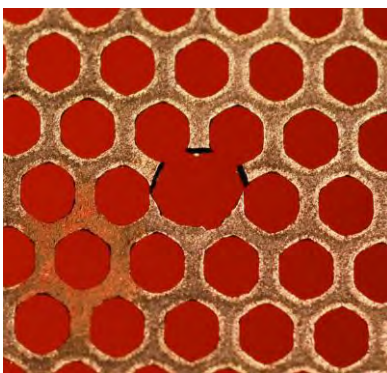


Figure 21. Close-up photo of the downstream face of the Decel grid showing a region of wear.

The erosion surrounding the apertures in a circular manner on the downstream face may be associated with barrel erosion due to charge exchange ions in this region. The upstream face showed indications of erosion in hexagonal patterns around each aperture.

Following the survey photo-documentation, the Accel grid was potted, sectioned and polished. The work on this grid is still continuing.

3. Decel Grid

Photographs of the downstream face and the upstream (flipped) face of the Decel grid are shown in Fig. 20.

A region of erosion in the lower left corner (6 to 10 O'clock) of the Decel grid was apparent. This partial ring may indicate greater erosion toward the outer radius of the grid. A close-up photograph of a region of the Decel grid that showed loss of webbing in a single aperture is shown in Fig. 21. This is approximately the same region shown for the Screen

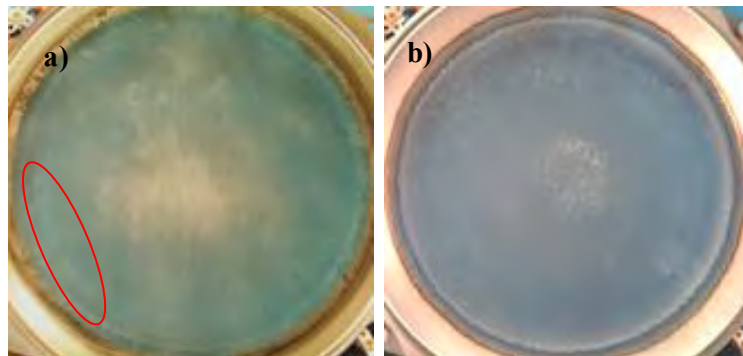


Figure 20. Downstream (a) and upstream (b) face of the Q2 Decel grid. An area of erosion (indicated in red) was noted.

As with the Screen grid, the potted, polished section of the Decel grid was then analyzed further using a Z-Scope. The erosion pattern of the Decel grid is presently being carefully analyzed. It is likely that changes in beam focusing due to ion density variations across the grid play a dominant role in the observed erosion pattern. Further work is being undertaken to evaluate this.

Finally a small section of the potted section was removed and used to obtain SEM images and elemental analysis of the grid and the deposit using EDS spectroscopy. The SEM images are shown in Fig. 23. EDS analysis showed that the deposit consisted solely of molybdenum that presumably originated from erosion of the Accel grid.

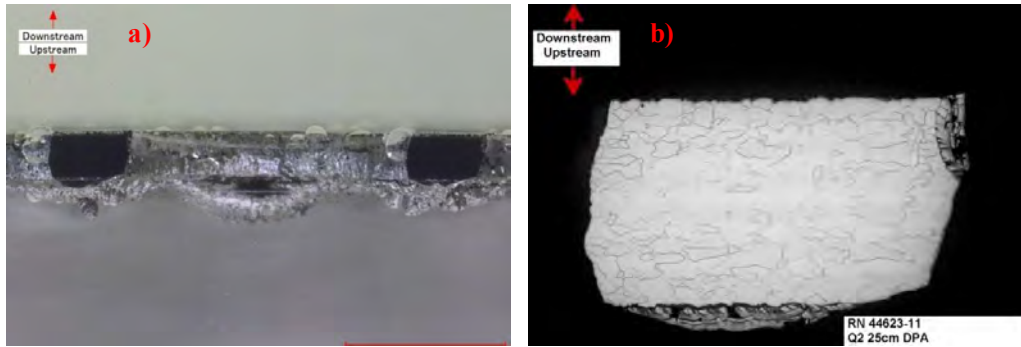


Figure 22. Example of optical (a) and metallographic (b) images of the webbing structure at the aperture mid-plane of the Q2 Screen Grid.

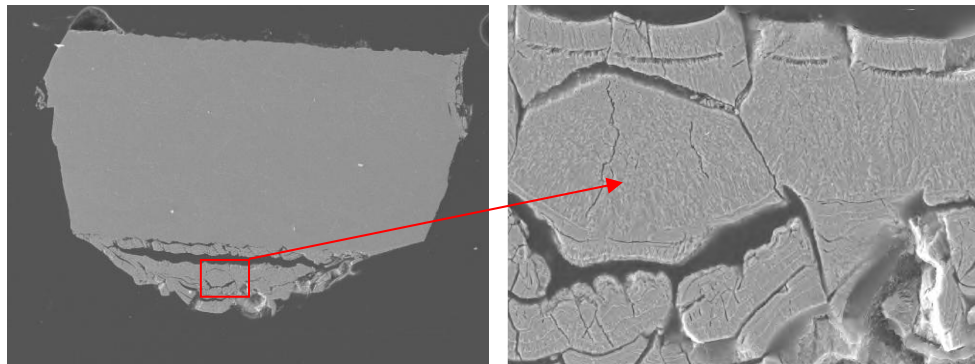


Figure 23. Low (left) and high (right) magnification SEM images of the deposit layer on the Q2 Decel Grid.

C. Discharge Cathode Assembly (DCA)

As was pointed out earlier, two DCAs were used during the 25 cm XIPS[®] thruster Life Test. The first DCA was operated for the entire High Power phase and through ~5000 hrs of the Low Power phase. At that point in the test an anomaly occurred that caused delayed starts. In order to continue the Life Test, it was decided to replace the entire DCA. The second DCA was identical in design to the first.

Although the second DCA was only used for the final 8000 hrs of the Low Power phase of the Q2 Life Test, it underwent a detailed DPA. The DCA was removed from the thruster and the Keeper was removed. Aside from a deposit of barium oxide that led to a discoloration of the ceramic, there was no indication of any significant changes.

The radiations shields were removed and photo-documented. The heater was then removed from the cathode tube and submitted for analysis. Optical and X-ray images showed little or no degradation.

The heater was then potted in epoxy and sectioned to allow further analysis of the interior through optical (Fig. 24) and metallographic images. Though some deterioration of the heater was apparent through minor discoloration of the MgO insulator, the heater was in very good condition.

The metallographic images show changes but no dangerous deterioration of the heater. There was some formation of tantalates and migration of tantalum into the MgO. A single coil (shown in Fig. 25) at the output end showed intrusion of the MgO into the outer conductor. While

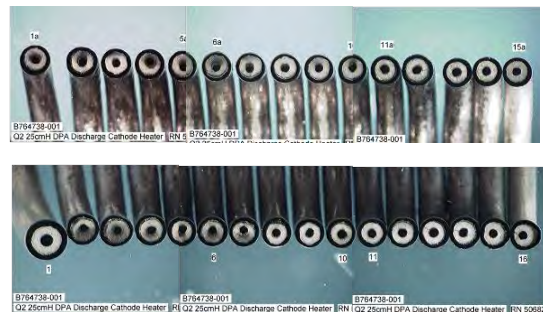


Figure 24. Optical images of the cross-sectioned DCA heater.

there was some loss of wall material, there was no danger of failure.

The Discharge Cathode Keeper was carefully removed, visually inspected and photographed. The End Cap was cut off so that any erosion effects on the end of the Keeper could be determined. Optical photographs of the Keeper End Cap are shown in Fig. 26. The original shiny appearance of the front of the Keeper End Cap has been abraded possibly due to plasma etching. Some minor discoloration and the presence of small black particles were noted on the backside of the Keeper End Cap.

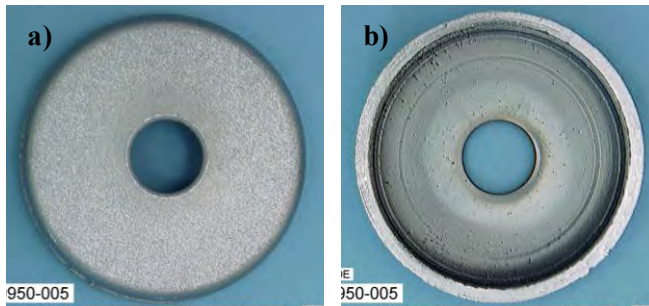


Figure 26. Photos of the front (a) and back (b) faces of the Q2 DCA Keeper End Cap.

smooth depression of the downstream face centered near the half radius location.

The Keeper aperture diameter increased by ~3% and the thickness reduced by a maximum of ~25% at a mid-radius location.

The Mo:Re Discharge Cathode Orifice Plate was then cut off from the Cathode Tube and analyzed using SEM/EDS. An overview and a higher magnification SEM image taken near the aperture on the front and rear faces of the Orifice Plate are shown in Fig. 28. Plasma erosion of the downstream (front) surface is apparent. The EDS spectrum of the downstream (front) surface is apparent. The EDS spectrum showed only rhenium and no molybdenum. The lack of molybdenum is presumably due to a higher sputter rate for molybdenum in this environment that has removed it from the surface. The presence of impregnant elements (barium and calcium) was noted and would be expected in this region of the cathode. The EDS spectrum and an elemental map (not shown) taken on the rear (upstream) face of the Orifice Plate showed the Mo:Re base material as well as the locations of barium and calcium on the surface.

ESCA data (not shown) taken on both the front and back faces of the orifice plate provided similar results to the EDS data for the elements present on the surface.

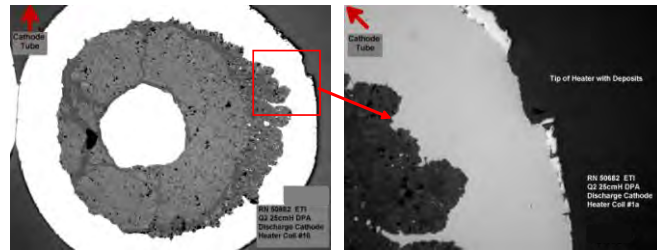


Figure 25. Metallographic image of one coil of the cross-sectioned DCA heater.

SEM/EDS analysis was then performed and showed only the presence of the original Mo:Re material that made up the Keeper and a small amount of barium as would be expected in this region of the cathode.

The Keeper End Cap was then potted, sectioned and polished. Optical and metallographic images of this cross-section are shown in Fig. 27. In this figure, 3 metallographic images have been placed side-by-side to create a complete image of the right side of the cross-sectioned Cap. Both this and the optical image show that only a moderate amount of erosion of the Keeper Face occurred. There is a

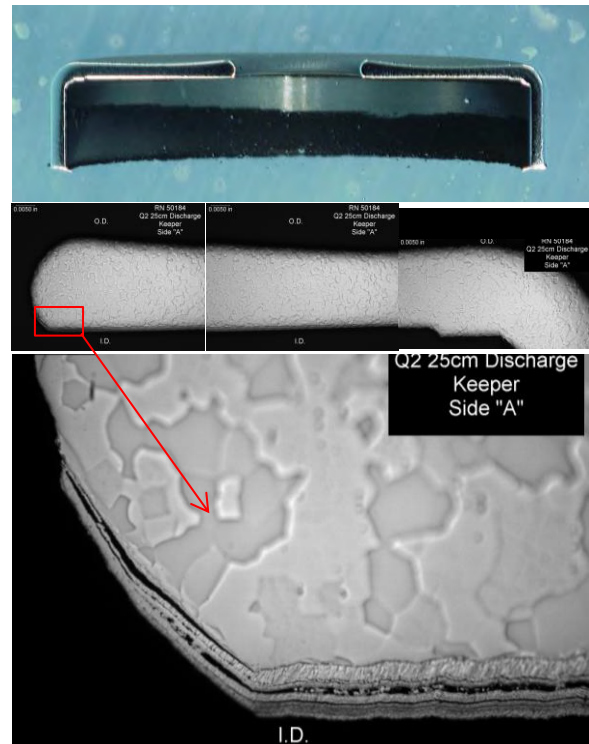


Figure 27. Optical (above) and Metallographic images of the cross-sectioned Q2 DCA Keeper Cap

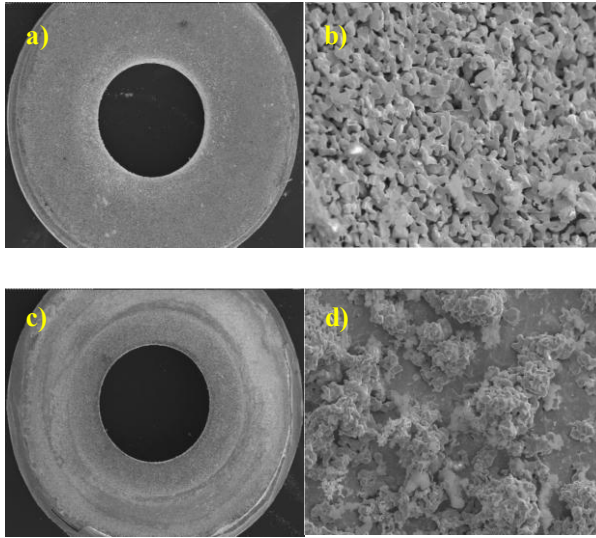


Figure 28. SEM images showing overview and high magnification images of the front (a & b) and the rear (c & d) of the DCA Orifice

The cathode insert is a hollow cylinder made of pressed porous tungsten and impregnated with Ba:Ca:Al₂O₃. During ignition the insert is heated (using the external, coaxial heater) and barium is freed and migrates from the pores to the inside surface of the hollow cathode where it evaporates. The barium eventually reaches and diffuses across the outside orifice plate where thermionic electron emission is used to ignite the cathode and eventually the main discharge. The depletion of barium has been considered a potential life limiting mechanism for the thruster. Careful analysis of the condition of the cathode inserts may provide some insight into this issue.

The DCA cathode insert was removed from the Cathode Tube, photographed, fractured into four sections and re-photographed. A single fractured section was selected, underwent ESCA and SEM/EDS analysis. It was then mounted and polished, and underwent SEM/EDS pore chemistry analysis.

Optical photographs are shown in Fig. 30. They show a white deposit on the outside surfaces consisting of bands, especially in the colder upstream region. The inside surface also consists of several bands or regions. In the forward, downstream region there is band of an apparent, white particulate residue. This residue becomes less dense in the central region. In the colder upstream region there are two distinct bands that have progressively darker appearance.

ESCA data was obtained but is not presented here. SEM images (low and high resolution) and EDS spectra were taken at 11 locations along the inner surface of the fragmented insert. The approximate locations are indicated in Fig. 31. The high resolution SEM images showed indications of “blooming” of the impregnant and the formation of tungstates at many locations on the surface. Changes in the morphology of the tungsten matrix from the cold, rear locations (region 2) to the hotter locations near the tip (region 11) can also be seen in Fig. 31.

The Discharge Cathode Orifice Plate was then potted, sectioned and polished. An optical image of the cross-section is shown in Fig. 29. There has been little or no erosion of the plate during the limited operating time. The “as-manufactured” taper of the orifice has been only slightly modified. A thin surface layer on the sidewalls and the downstream face (plasma exposed regions) indicates a modification of the surface, possibly due to the higher sputter rate of molybdenum from the Mo:Re base material. Metallographic images for the right side of the cross-section are included in Fig. 29. The images clearly show surface modification due to plasma interaction. A thin layer has been produced possibly through differential sputtering rates, diffusion of impregnant material, and heating.

The orifice plate aperture diameter was basically unchanged while erosion of the face reduced the thickness at the center by ~ 15% near the start of the original tapered portion of the orifice.

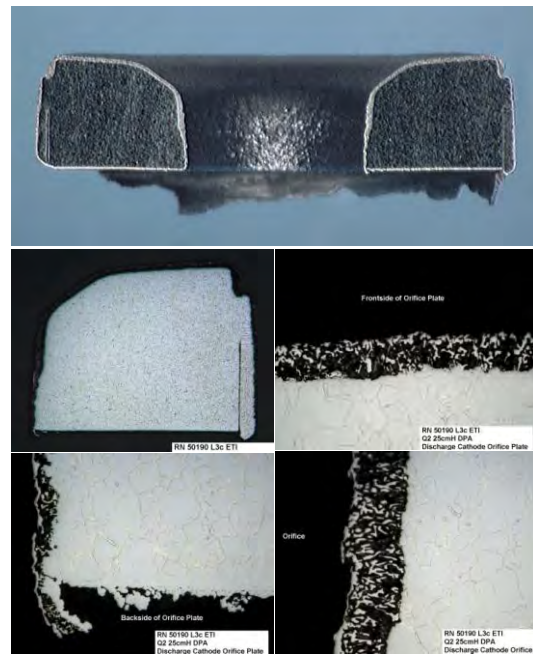


Figure 29. Optical (upper) and Metallographic images of the cross-sectioned Q2 DCA Orifice Plate

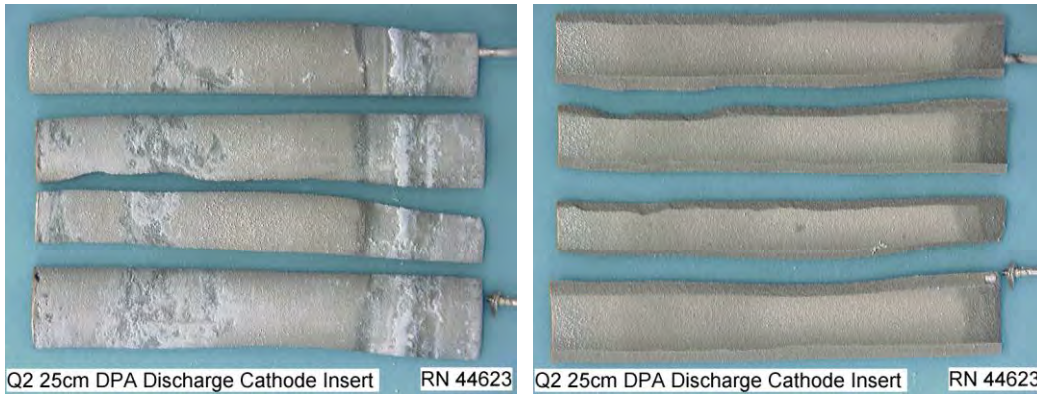


Figure 30. Photographs of the outer (a) and inner (b) sides of the Q2 DCA hollow cathode insert after intentional fracturing for DPA. The downstream region is to the left and the upstream to the right.

EDS data taken across the inside diameter of the insert can be summarized as follows. In the upstream location (regions 1 and 2) there is very little heating of the insert either during ignition (with the heater activated) or operation. The SEM photographs in this location show little or no change from a non-operated insert. In the central position (region 4 to 8) heated during ignition and operation but having little or no interaction with the plasma, there is a reduction in the amount of barium. In the downstream location (regions 9 to 11), there is significant depletion of barium and the presence of molybdenum. The molybdenum signal is first detectable around region 7 but is seen to grow from region 9 to 11. This surface sees significant plasma interaction during operation and molybdenum arising from erosion of the orifice plate may have been deposited in the downstream region of the insert.

The fractured insert section was then potted in epoxy, polished and returned to SEM/EDS for pore analysis. In this case the cross-sectioned insert is examined and EDS spectra generated from within a single pore of the pressed tungsten matrix. The purpose is to obtain a measure of the barium content in the insert as a function of both axial and radial position. From this a determination of the degree to which barium has been depleted and the areas from which it has been depleted may be made. A difficulty associated with this determination is the inability to discern the percentage of barium that is free and that which has been chemically bonded to tungsten in the formation of barium tungstates.

An extensive amount of data is accumulated in performing this “pore analysis”. Lower magnification (400x) SEM images provide overviews of the various locations. Higher magnification (2000x) images of the polished pores show details of the pore structure and content. Only samples of the data will be provided here.

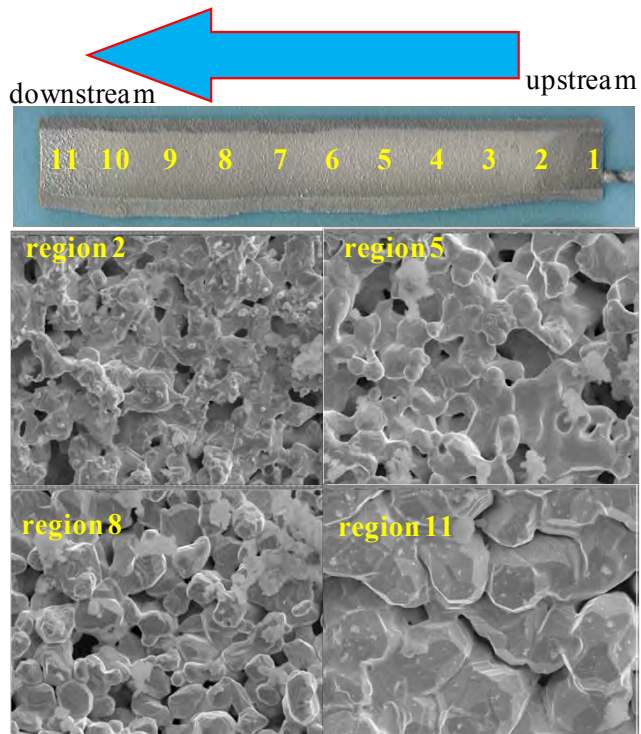


Figure 31. Regions of inner diameter of Q2 DCA insert that underwent SEM/EDS analysis and SEM images from specified regions.

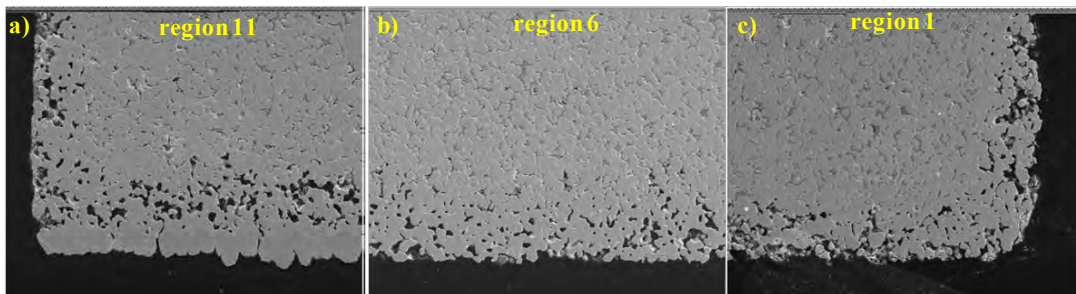


Figure 32. Overview SEM images of the inner diameter region of the cross-sectioned Q2 DCA insert. Images show the downstream (a), central (b) and upstream (c) regions of the insert.

Figure 32 shows overview SEM images of the inner diameter of the insert in 3 locations; the “downstream” location which reaches temperatures >1200 C and undergoes plasma interaction during operation, a middle location which gets hottest during ignition, is significantly cooler during operation and is not expected to interact with the plasma (at least early in life), and the rear “upstream” location which is relatively cool during life and would not be expected to undergo significant changes.

With lower resolution SEM images there appears to be a greater amount of dark (open) pores in the downstream end, both on the front face and toward the inner diameter. In addition, in this front location, at the inner diameter edge, there appears to be a region of denser material. An elemental map (Fig. 33) of this area indicates that this region contains molybdenum. The source of this molybdenum (also noted with EDS data taken on the unpolished inner diameter surface) is likely to be the front face of the orifice plate where preferential loss of the molybdenum was observed. The molybdenum could be incorporated into the plasma that exists in this region during operation and subsequently diffuse into this part of the insert.

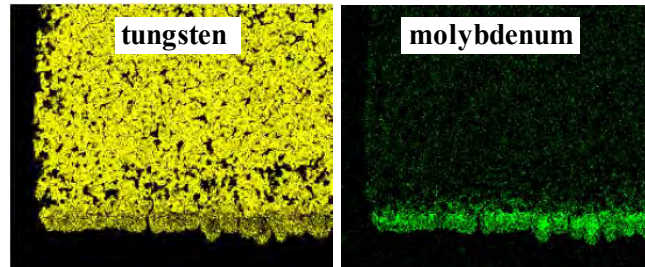


Figure 33. Elemental map of at the exit region of the insert showing the molybdenum layer on the inner surface.

High resolution SEM images, shown in Fig. 34, show the changes to the contents of the pores in regions, taken closest to the insert inner diameter, at the downstream (a), middle (b) and upstream (c) locations. The EDS data was obtained at 11 axial locations along the mid-radius and in 5 radial locations in the downstream, middle and upstream locations. Of the more than 23 pores examined, the only significant change in elemental content was found in the pore examined in the front, inner diameter region. Here the barium level had dropped from a typical level by $\sim 25\%$, while the calcium level dropped to the noise level.

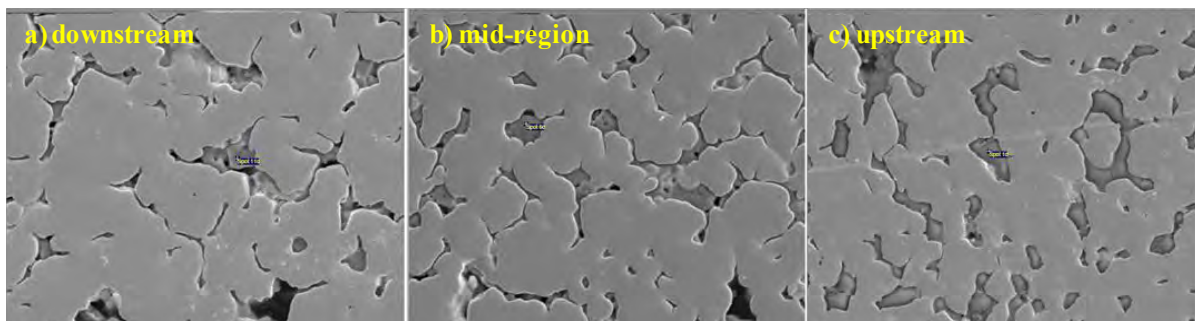


Figure 34. High resolution SEM images used in performing pore analysis in both axial and radial directions of the cross-sectioned Q2 DCA Insert.

D. Neutralizer Cathode Assembly (NCA)

Upon inspection of the Q2 thruster following the completion of the Life Test, it was immediately noted that a region surrounding the NCA Keeper End Cap orifice consisted of thin, flaky material. Ultimately, the flaky material was lost.

The NCA was removed from the thruster and the Keeper was detached. Very slight discoloration of the ceramic was noted. The radiation shields were removed and photo-documented. The heater was then removed from the cathode tube. Optical and X-ray images showed little or no degradation of the heater.

The heater was then potted in epoxy, sectioned, and polished. Optical (Fig. 36) and metallographic (Fig. 37) images were taken. Though some deterioration of the heater was apparent through minor discoloration of the MgO insulator, the heater appeared to be in good condition.

In a few coils the metallographic images showed a significant formation of tantalates and migration of tantalum into the MgO. There was some degree of tantalate formation in almost every coil, generally as a ring, or partial ring, around the inner conductor. Although MgO had penetrated into the outer conductor in many coils, wall material was not reduced to the point of a potential failure. In general the heater appeared to be in good to fair condition.

The Neutralizer Cathode Keeper was carefully removed, visually inspected and photographed. The end cap was cut off so that any erosion effects on the end of the Keeper could be determined. Optical photographs of the Keeper and its Cap are shown in Fig. 38. The original shiny appearance of the front of the Keeper End Cap has been abraded due to plasma etching. The Keeper orifice has been significantly enlarged due to erosion and there is a large curved blemish seen in the upper portion of the front of the End Cap. The inside of the Keeper End Cap shows the several bands of discoloration and apparent deposition.

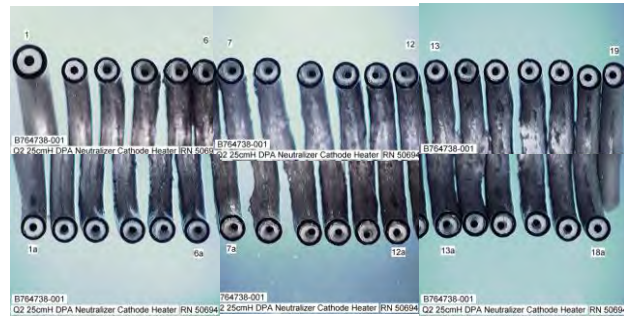


Figure 36. Optical image of cross-sectioned Q2 NCA heater.

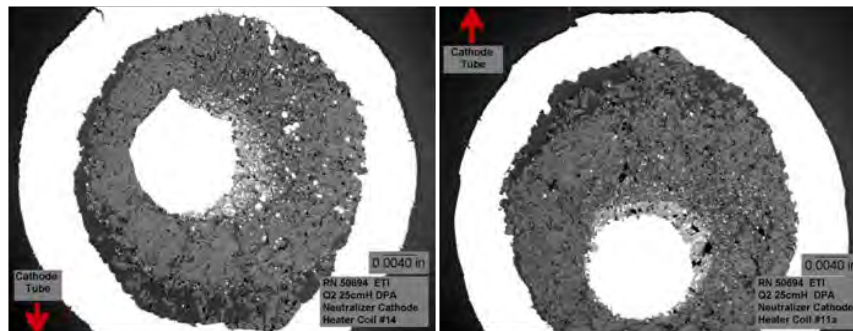


Figure 37. Metallographic images of the Q2 NCA Heater Coil cross-section.

A detailed SEM/EDS analysis was then performed on the front and back sides of the Keeper End Cap. Low and high magnification SEM images taken over 8 areas on the front “downstream” side of the Keeper documented the entire surface and showed the irregular edge of the orifice, the granular nature of the surface and the presence of dark particles. Some of these features can be seen in Fig. 39. EDS data showed the Mo:Re base material. In addition, chlorine, potassium, sodium and the impregnant materials, barium and calcium, were present in the particulate. Aside from the impregnant material, the origin of these elements is unclear.

The back face or inside “upstream” surface of the Keeper End Cap was then documented in a similar manner. Typical SEM images are provided in Fig. 40. These images indicate some deposition

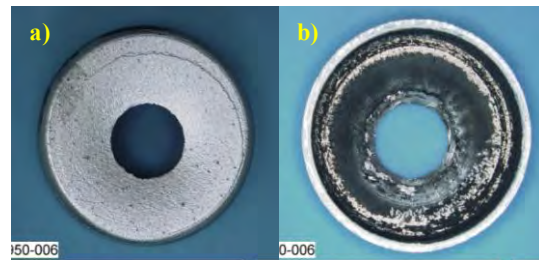


Figure 38. Photos of the front (a) and back (b) faces of the Q2 NCA Keeper End Cap.

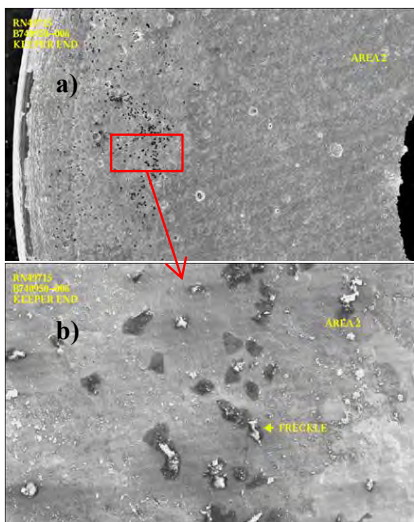


Figure 39. Low (a) and high (b) magnification SEM images showing presence of particulates on the front face of the Q2 NCA Keeper.

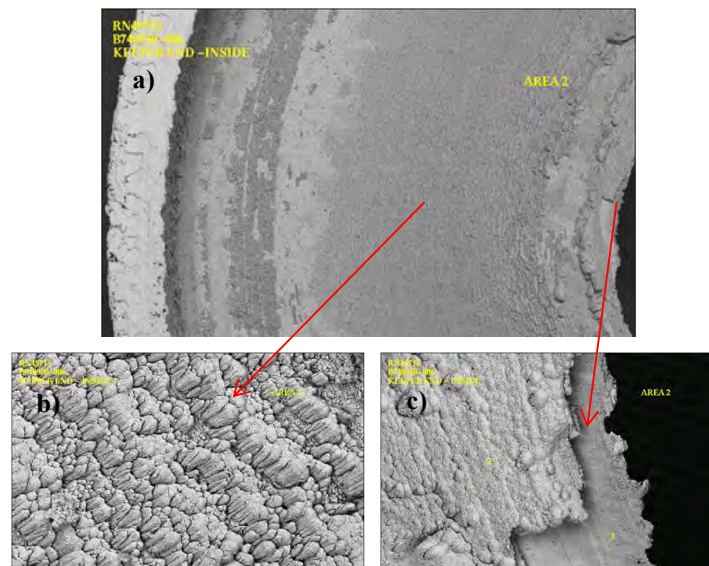


Figure 40. Low (a) and high (b & c) magnification SEM images showing deposit and orifice edge on the back face of the Q2 NCA Keeper.

but little erosion as machining marks were still visible. There are “rings” of deposit and the orifice edge is irregular due to the loss of material. The outer ring in these images is the outer wall of the Keeper tube from which the End Cap has been removed. In the high magnification SEM image the orifice edge and a columnar deposit are apparent. From EDS analysis the only elements present on the back surface of the NCA Keeper Cap were the base Mo:Re material and barium and calcium from the insert impregnant.

The Keeper End Cap was then potted, sectioned and polished. Optical and metallographic images of this cross-section are shown in Fig. 41. Three metallographic images have been placed side-by-side to create a complete image of the right side of the cross-sectioned End Cap. It is clear that significant erosion of the Keeper Face has occurred. The thickness of the End Cap has reduced in a nearly linear manner from the outside to the orifice, producing a knife-edge at the remaining orifice. From the optical image, the erosion seems to have occurred on the outer (“downstream”) surface. Along the inner (“upstream”) surface there is a ribbon-like structure that may have become attached as portions of the orifice eroded and flaked off.

SEM/EDS analysis was performed on the potted, polished section of the NCA Keeper Cap. EDS along the cross-section showed Mo:Re base material only. The ribbon-like deposit was similar but also contained barium.

The Keeper aperture diameter approximately doubled in size while the thickness of the End Plate reduced by a third on the outside to a “knife-edge” at the orifice.

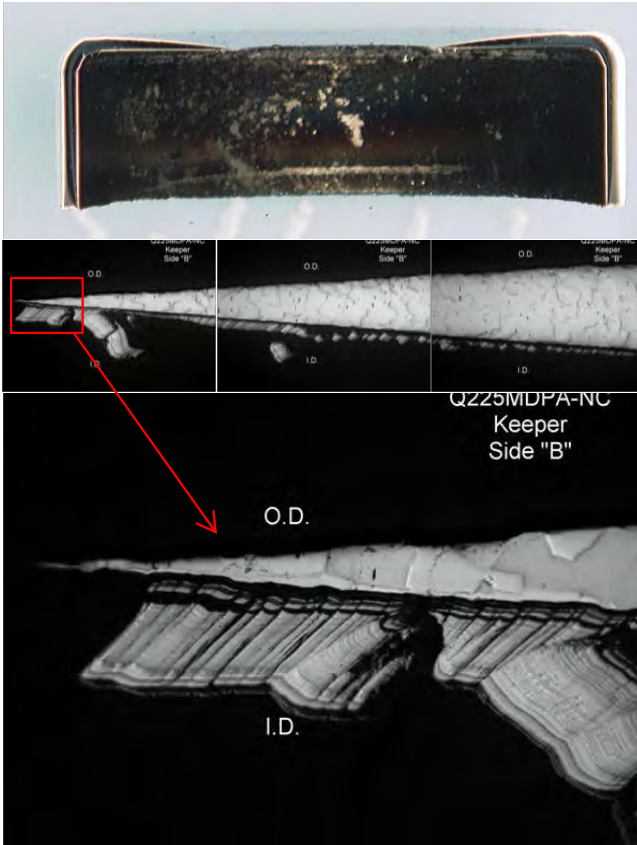


Figure 41. Optical (above) and Metallographic images of the cross-sectioned Q2 NCA Keeper Cap

the clear identification of impregnant materials from the Cathode Insert: barium, calcium and aluminum along with tungsten.

Following removal of the heater, the cathode tube was removed and photographed. The NCA Orifice Plate was then cut off the tube and analyzed using SEM/EDS.

An overview and a higher magnification SEM images taken near the aperture of both the front and the back of the Orifice Plate are shown in Fig. 42. On the front (downstream) surface the plasma eroded surface texture is apparent. As with the DCA Orifice, the EDS analysis showed a strong presence of rhenium and a lack of molybdenum. Unlike the DCA Orifice there was no presence of impregnant elements (barium and calcium) in this region. SEM/EDS analysis of a region on the outer diameter of the front face was similar though the high magnification SEM image showed somewhat different morphology. An elemental map, for a region on the outer diameter of the front face of the Orifice Plate is shown in Fig. 43. The different morphology and the dominant presence of rhenium at this location on this surface are clear.

Optically, the rear (upstream) face of the Orifice Plate had a shiny inner and a dark outer ring. On the inside diameter, the EDS analysis showed only the base materials of molybdenum and rhenium. There was also some indication of the presence of tungsten on the surface. At the outer diameter the SEM image showed the presence of a deposit and the EDS analysis showed

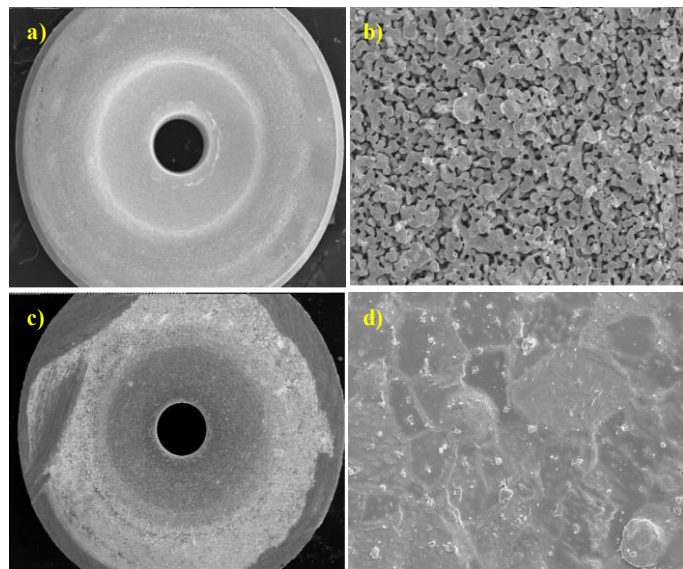


Figure 42. SEM images showing overview and high magnification images of the front (a & b) and rear (c & d) of the NCA Orifice Plate.

The Neutralizer Cathode Orifice Plate was then potted, sectioned and polished. An optical image of the cross-section is included in Fig. 44. There has been significant erosion of the plate over the duration of the Life Test resulting in a dishing of the original flat disk and asymmetric widening of the orifice walls. Metallographic images for the right side of the cross-section are also shown in Fig. 44. The images clearly show surface modification due to plasma interaction. As with the DCA a thin surface layer has been produced.

The original orifice plate aperture had straight walls. It has now become significantly dished on the downstream side. On the upstream side the orifice plate aperture diameter has not changed but on the downstream end the maximum diameter of the dished region has more than tripled. At the base of the dish, the orifice plate has thinned to approximately half of its original thickness.

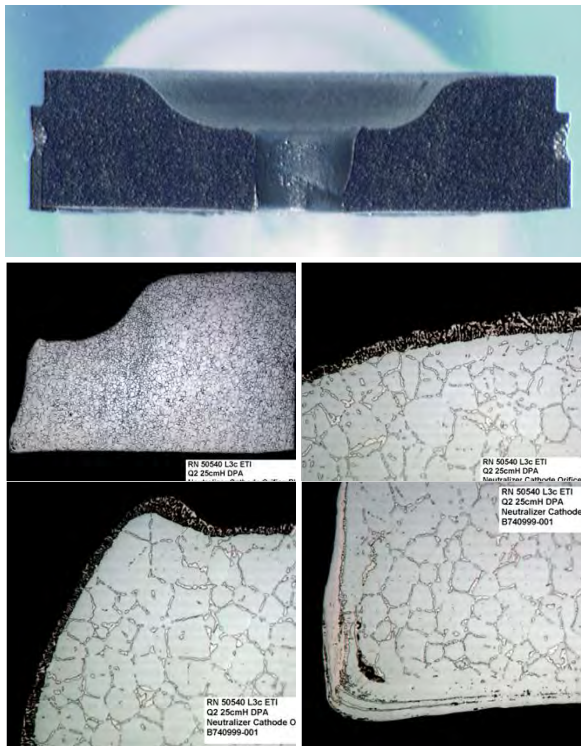


Figure 44. Optical (upper) and Metallographic images of the aperture side wall, and higher magnification images of the top surface, and the upper and lower portions of the side wall of the cross-sectioned Q2 DCA Orifice Plate.

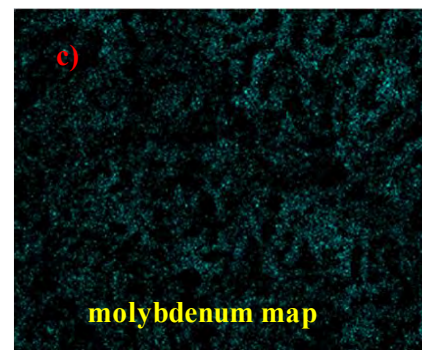
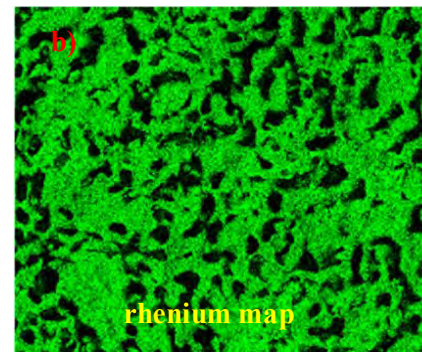
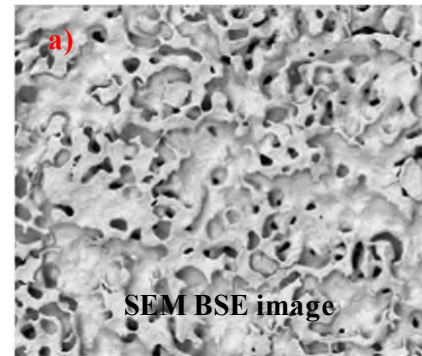


Figure 43. SEM image (a) from the outside radius of the front face of the NCA Orifice Plate and EDS elemental maps (b & c)

The NCA cathode insert was removed from the Cathode Tube and the outside surfaces were photographed. The hollow insert cylinder was then fractured into four sections. A single fractured section was selected, underwent ESCA, imaged using SEM, mounted and polished, and finally underwent EDS pore chemistry analysis.

Optical photographs are shown in Fig. 45. The outside surfaces show signs of scoring possibly due to adherence to the cathode tube and caused during removal of the insert. The inside surface consists of several bands or regions.

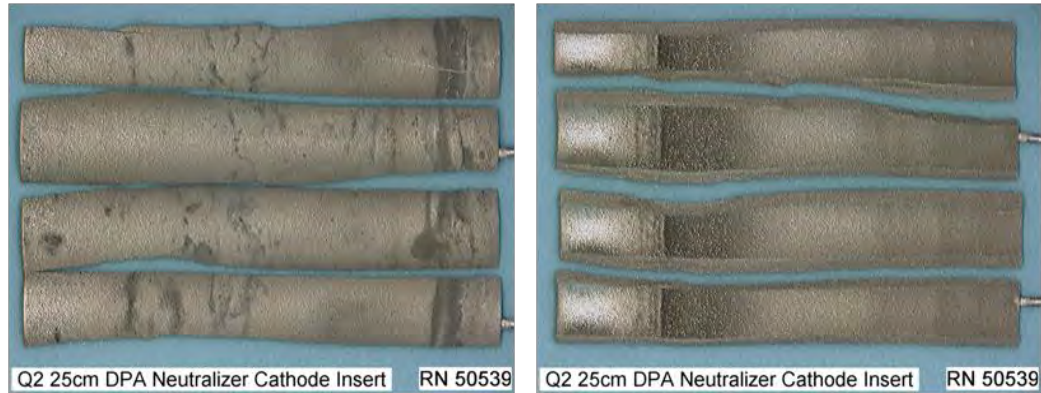


Figure 45. Outer (a) and inner (b) photographs of the Q2 NCA hollow cathode insert after intentional fracturing for DPA.

In the forward, downstream end there is a relatively dense band of an apparent, white particulate residue. This transitions to a dark region with much less white residue. The central region is a lighter grayish area. In the upstream (cold) region there are less distinct bands that have progressively darker appearance.

ESCA data was obtained at three locations on both the inside and outside of the insert. SEM images (low and high resolution) and EDS spectra were taken at 11 locations along the i.d. surface of the fragmented insert. The approximate locations are indicated in Fig. 46. Moving from the cold rear region of the insert to the hot front, changes in the morphology of the insert surface are clear in the high resolution SEM images. Re-deposition in the back upstream region, relatively unchanged structures in the middle region and depletion in the front can all be seen.

In the upstream location (regions 1 and 2) the SEM photographs show little or no change from a non-operated insert. In regions 3 and 4 the barium content has reduced but from region 5 to 11 there is little or no indication of barium on the surface. As with the DCA insert, molybdenum is detected in the

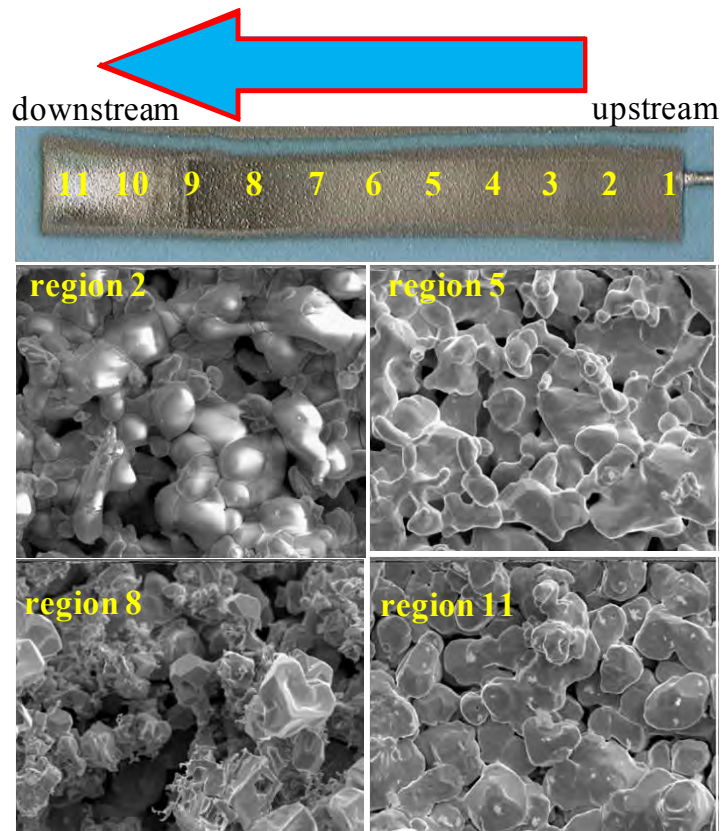


Figure 46. Regions of inner diameter of Q2 NCA insert that underwent SEM/EDS analysis and SEM images from specified regions.

downstream region of the insert.

Figure 47 shows overview SEM images of the inner diameter of the insert in 3 locations; the “downstream” location which reaches temperatures of ~ 1150 °C and undergoes plasma interaction during operation, a middle

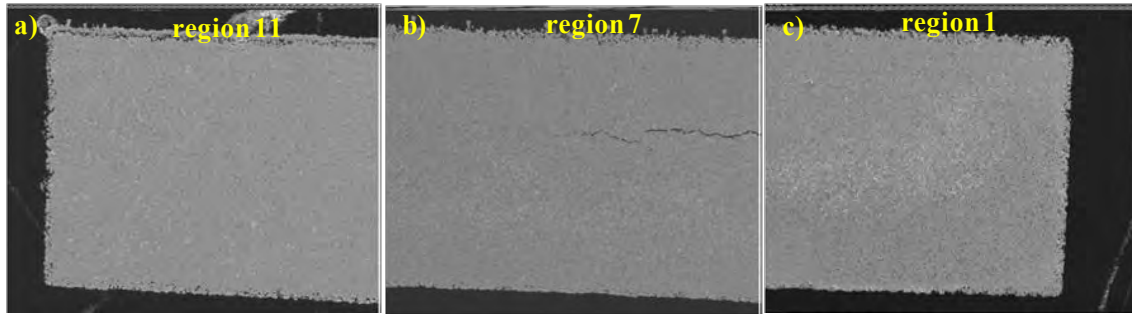


Figure 47. Overview SEM images of the cross-sectioned Q2 NCA insert. Images show the downstream (a), central (b) and upstream (c) regions of the insert.

location which gets hottest during ignition, is significantly cooler during operation and is not expected to interact with the plasma (at least early in life), and the rear “upstream” location which is relatively cool during life and would not be expected to undergo significant changes.

As with the DCA insert, there appears to be more dark (open) pores in the downstream end, both on the front face and toward the inner diameter than in the middle or the upstream regions. In addition, in this front location, at the inner diameter edge, there appears to be a region of denser material which is likely molybdenum. The apparent zone of depletion on the outer diameter of all three regions suggests that impregnant has been lost in spite of the close proximity of the insert to the cathode tube.

High resolution SEM images, shown in Fig. 48, show the changes to the contents of the pores in regions, taken closest to the insert inner diameter, at the front (a) downstream, middle (b) and rear (c) upstream locations. Of the more than 23 pores examined, the only significant change in elemental content was found in the pore in the region closest to the downstream end of the insert and closest to the inner diameter. The barium level in this region dropped $\sim 40\%$ while the calcium level dropped to the noise level.

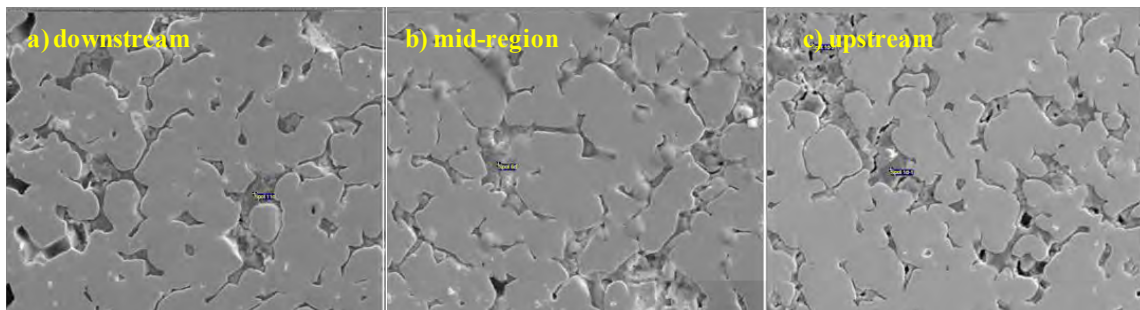


Figure 48. High resolution SEM images used in performing pore analysis in both axial and radial directions of the cross-sectioned Q2 NCA Insert.

E. Additional Analysis and Documentation of Other Sub-Components

Although the emphasis of the Q2 evaluation and of this paper was on the grid optics and the cathodes, every sub-component of the Q2 thruster was very carefully inspected, investigated and documented to ensure that there were no potential issues that would impact mission or performance. Additional findings were relatively small.

Molybdenum flakes were found to have accumulated to a small degree in and around the discharge chamber. It was unclear if these flakes were present during the Life Test or if they had been freed up due to post Life Test handling. The upper section of the anode liner, as was intended, had captured a significant amount of molybdenum and may have been the origin of some of these flakes. Grid shorts that may have been caused by such loose flakes did occur during the Life Test but were easily cleared either by thermal cycling or using Grid Clearing circuitry available with the XPC.

The High and Low voltage propellant isolators were carefully studied and found to be in excellent condition. The magnetic field within the discharge chamber was remapped and while a decrease in field strength was found, there was no evidence of this having any impact on performance.

Wiring and power connectors are still being examined but there have been no significant findings to date.

F. Conclusions

Having completed its Life Test, the Q2 25 cm XIPS[®] Thruster successfully met all requirements of the orbit-raising and station-keeping missions for the Boeing 702 class geosynchronous, communication satellite. The Life Test was terminated voluntarily after operating for total of 16,250 hrs, 14,142 cycles and processing 158 kG of xenon.

Subsequent to the completion of the Life Test the status of the thruster was carefully documented by a series of very detailed non-destructive and destructive physical analyses. These test included electrical tests, weight measurements and photo-documentation of every sub-component of the thruster as it was disassembled. DPA was performed on the optics assembly and both the discharge and the neutralizer cathodes. No potential points of failure were identified. There was noticeable wear in the central portion of the Screen grid that was likely due to the operation at high discharge voltage. The NCA Keeper eroded more than was expected and while it operated without issue throughout the Life Test, investigations are on-going to determine the cause of this erosion and to provide modifications to this component and/or its operation in order to meet more stringent mission requirements [8].

L-3 ETI is the largest supplier of electric propulsion systems in the world. With more than 130 units and about 270,000 hrs accumulated in orbit, the XIPS[®] thruster has an extensive and unique flight heritage.

Acknowledgments

The authors would like to acknowledge the technical support of many colleagues (present and former) at L-3 ETI including Tom Bond, Brian Buckley, Jack Colby, Robert Guerrero, Steve Hart, Julio Hurtado, Eric Nelson and Chris Reed. Brandon Smith (GA Tech), a summer intern at L-3 ETI, has been responsible for much of the preparation and analysis of the potted, polished and sectioned Grid Optics. We would also like to acknowledge Dr. Dan Goebel and his colleagues at JPL who have done significant work in testing, analyzing and modeling the 25 cm XIPS[®] thruster to qualify it for use in NASA missions. Finally some of this work was guided by Dr. Garnick Hairapetian, now with the Boeing Satellite Development Center.

References

- ¹K-R.Chien, S. Hart, W.G. Tighe, M. DePano, T. Bond, and R. Spears, “L-3 Communications ETI Electric Propulsion Overview,” *29th International Electric Propulsion Conference*, Princeton, IEPC-2005-075, Oct., 2005.
- ²W.G. Tighe, K-R. Chien, D.M. Goebel, and R.T. Longo, “Hollow Cathode Ignition Studies and Model Development,” *29th International Electric Propulsion Conference Proceedings*, Princeton, IEPC-2005-314, October, 2005.
- ³W.G. Tighe, K-R. Chien, D.M. Goebel, and R.T. Longo, “Hollow Cathode Emission and Ignition Studies at L-3 ETI,” *30th International Electric Propulsion Conference Proceedings*, Florence, IEPC-2007-023, September, 2007.
- ⁴D.M. Goebel, J.E. Polk, I.G. Mikellides, J.R. Brophy, W.G. Tighe, and K-R. Chien, “Evaluation of 25-cm XIPS[®] Thruster Life for Deep Space Mission Applications,” *31st International Electric Propulsion Conference*, Ann Arbor, IEPC-2009-152, September, 2009.
- ⁵W. G. Tighe, K. Freick and K-R. Chien, “Performance Evaluation and Life Test of the XIPS Hollow Cathode Heater”, *AIAA-2005-4066*, 41th Joint Propulsion Conference, Tucson, AZ, July 10-13, 2005.
- ⁶J.E. Polk, D.M. Goebel and W. Tighe, “A Long Duration Wear Test of a XIPS[®] 25-cm Thruster Discharge Cathode,” *31st International Electric Propulsion Conference*, Ann Arbor, IEPC-2009-017, September, 2009.
- ⁷A.Sengupta, J. Brophy, J. Anderson, C. Garner, K. de Groh and C. Karniotis, “Summary of 30,000 Hr Life Test of Deep Space 1 Flight Spare Ion Engine,” *41st AIAA/ASME/SAE/ASEE Joint Propulsion Conference Proceedings*, Tucson, AIAA-2005-4397, July, 2005.
- ⁸D.M. Goebel, I.G. Mikellides, J.E. Polk, J. Young, W. Tighe and K-R. Chien, “Keeper Wear Mechanisms in the XIPS[®] 25-cm Neutralizer Cathode Assembly,” *31st International Electric Propulsion Conference*, Ann Arbor, IEPC-2009-153, September, 2009.